Chapter III

Modification of aggregation characteristics of cationic surfactants by hydroxy aromatic derivatives of naphthalene under salt-free condition

1. Introduction

Ever since the interests are generated in scientific community on micellar shape transition phenomenon and the formation of long wormlike micelles (WLM) more than 40 years ago, a number of triggering agents for tuning the micellar surface curvature leading to sphere to rod transition, especially those of cationic micelles, have been in the center of attention. Some of these agents are highly efficient compared to others. For some cationic surfactants, wormlike micelles are formed even at low salt concentrations by using specific strongly binding aromatic anions, such as salicylate, tosylate, chlorobenzoate and naphthalene sulfonate. The research on WLM has drawn considerable interest because its rheology is challenging due to the presence of multiple pertinent length scales and stress relaxation mechanism. This relatively new material has many applications using that of fractured fluids in the oil field, efficient drag reducing agent in hydrodynamic engineering and home care; personal care and cosmetic products. A large number of study in micellar shape transitions in cationic, anionic and catanionic surfactant systems have been reported in the literature, but almost all the investigations engaged organic and inorganic salts and involved charge screening of the head groups via electrostatic interactions. Surprisingly, attempt to promote micellar morphology transition under salt-free condition is meagre in the literature.

Organic π-conjugated molecules are effective tuners in the formation of various nanostructural materials and the entailed route is potentially facile and efficient for the development of functional materials of technological and biological importance. Microstructural transitions of micellar aggregates, especially the nature of transition from normal spherical micelles to long wormlike micelles mediated by organic π-electron systems are of fundamental scientific interest and have been reported recently. It has been shown that along with hydrophobic interactions, cation-π interaction is principally involved and the success of 1 and 2 Naphthols in effecting microstructural

transition of micelles like CTAB and CPB lies also in their unique ability to form H-bonds with interfacial water molecules, which have shown unusual H-bond donating properties compared to bulk water.

Studies on the effect of neutral naphthols and methoxynaphthalenes on CTAB micelles that showed the formation of cylindrical micelles with the former but not the later point to the importance of the hydroxyl (OH) group of salicylate molecules as well. It is argued that the cation-π interaction is one of the most important driving force in tuning the surface curvature via charge screening of the head group in the case of salicylate promoter as well. 1 and 2 Naphthols triggered wormlike micelle formation on CTAB and CPB. However, in the case of salicylate, it is believed that the ionized salicylate molecules are positioned in an inner location of the micelle-water interfacial region (palisade layer) for effective electrostatic interaction between the cationic head group of surfactant molecule and COO^- group of salicylate molecule. It has further been argued that with decreasing pH and consequent protonation, salicylate molecules are positioned at an outer location of the micelle water interface with the cationic head group perpendicular to their π-face, resulting in stronger cation-π interaction. In general, these studies bring new fundamental insight into the driving molecular forces behind wormlike micelle formation in cationic surfactant/hydrotopes solutions (including 1 and 2 Naphthols), showing that in addition to the hydrophobic effect and electrostatic interactions, the importance of H-bonding and cation-π interactions are also vital importance. Further investigations might provide deeper insights into the molecular mechanism through which H-bonding and cation-π interactions contribute to the equilibrium microstructure and associated rheological behavior of cationic surfactant-hydrotrope mixtures.

Interests in the micellar morphology transitions in presence of organic π-conjugated systems as above also stem from another important point of view; the biological relevance of cation-π interaction and the fact that the self-assembled aggregates of surfactants viz., micelles, vesicles etc. are considered as simple models of biological membrane including cell membranes. It is indeed interesting to further note that in structural biology, the importance of quaternary ammonium ion is well recognized. For example, Dougherty and co-workers found that the anionic cyclophane (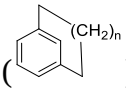

) is a

better receptor for quaternary ammonium and iminium ions in aqueous borate buffer than for corresponding neutral molecules.

Some of the strongest support for cation-π interactions at acetylcholine binding sites comes from studies of the nicotinic acetylcholine receptor (nAChR). Even without an X-ray structure, the evidence for a key role for aromatic residues at the ACh-binding site, and hence for the possible involvement of a cation-π interaction, is very strong.

Further, biological membranes exhibit various function-related shapes, and the mechanism by which these shapes are created is largely unclear. It is generally believed that the changes of membrane topology is produced as a result of a complex interplay between membrane proteins, lipids and certain physical forces. In view of the abundance of zwitterionic phosphatidylcholine in biomembranes and the ubiquitous feature of transmembrane proteins to localize aromatic aminoacids near the membrane-water interface, present study on the interaction of cationic head groups with aromatic π-systems definitely add to the understanding the tuning of surface curvature of biophysical membranes in presence of transmembrane proteins.

From the ongoing discussion it is amply clear that a completely new driving force is operational viz., cation-π interaction in presence of cationic head group (including quaternary ammonium ion (CTAB)) and the π-electron face of aromatic π-system along with hydrophobic interaction and H-bonding. This lead to highly efficient tuning of surface curvature of cationic micelles resulting in sphere-to-rod/ wormlike micelles transitions under salt-free condition. As have been already mentioned, further study would contribute to the deeper insights into the molecular mechanism by which H-bonding and cation-π interaction lead to the microstructure transition of micellar aggregates. Surprisingly, only a few works in this direction are reported.

In the present chapter, a detailed study of the interaction of CTAB and CPB micelles with the aromatic systems viz., 1 Naphthol, 2 Naphthol and 2,3 Dihydroxynaphthalene (2,3 DHN) have been undertaken along with the subsequent microstructural transition from spherical to WLM. Molecular level picture have been obtained from 2D NMR study. The morphology transitions have been investigated by means of SANS and the detail rheological aspects have been explained dynamic rheological investigation.

2. Materials and Methods

Materials

Cetylpyridinium bromide (CPB) and Cetyltrimethylammonium bromide (CTAB) were purchased from Across chemicals (USA) and was used as received. 1 and 2 Naphthols (Fluka, Germany) and 2,3 Dihydroxynaphthalene (Fluka, Germany) were further purified by vacuum sublimation followed by crystallization from 1:1 aqueous methanol. Methanol was distilled prior to use. Double distilled water (conductance below 2 μS/cm, pH ~6.5-7) was used for all experimental purposes. D_2O was purchased from Aldrich, USA (Purity >99.9%).

Methods

2.2.1. Specific conductivity measurements- The specific conductivity measurements were carried out in Metler Toledo Digital Conductivity bridge (MC226) (accuracy 0.1%) using a dip-type immersion cell with cell constant 1.0 (±0.05) cm^{-1}. 5 min equilibrium time was allotted before each reading. Constant temperature was maintained during the experiments with Remi ultra-thermostat (CB-700) with precision ± 0.1K. The uncertainty of the measurements was ±0.01μS.cm^{-1}.

2.2.2. Small Angle Neutron Scattering (SANS). The SANS measurements were carried out using small angle neutron scattering diffractometer at the Dhruva reactor, Bhabha Atomic Research Centre, Trombay, India. The diffractometer uses a beryllium oxide filtered beam with a mean wavelength (λ) of 5.2 Å. The angular distribution of the scattered neutrons is recorded using a one-dimensional (1D) position-sensitive detector (PSD). The accessible wave vector transfer ($Q = 4\pi \sin\theta/\lambda$, where 2θ is the scattering angle) range of the diffractometer is 0.017-0.35 $Å^{-1}$. The PSD allows simultaneous recording of data over the full Q. The samples were held in a quartz sample holder of 0.5 cm thickness. The measured SANS data have been corrected and normalized to absolute unit (as cross-section per unit volume), using standard procedures.

2.2.3. Nuclear Magnetic Resonance Spectroscopy (NMR). ^{1}H-NMR experiments were performed in Bruker (Germany) ADVANCE spectrometer operating at 300 MHz frequency (for characterization) and at 600.13 MHz for 2D Nuclear overhauser spectroscopy (NOESY) study. Signals are quoted as δ values in ppm using residual

protonated solvent signals as internal standard (D_2O: δ 4.79 ppm). Respective solutions were made in D_2O and 0.6 mL of the same was used for each measurement. Data are reported as chemical shift. 2D NOESY spectra was studied using Brucker standard software acquisition program noesyphpr in phase-sensitive mode using 5 mm BBO probe. An acquisition time of 0.085 sec and relaxation delay of 2 sec was used between the scans. The mixing time was 300 milisec. A total number of 2048 complex point were collected. Number of 16 scans were undertaken.

2.2.4. Rheology. The rheological experiments were done using cone-plate geometry with 4^0 truncation angle, with diameter 25 mm and 0.105 mm sample gap in MCR 302 (Anton Paar, Germany) equipped with Peltier temperature control system. The samples were initially stirred at 60^0C for three hours for homogenization and equilibrated for 72 hrs. During measurement, samples were equilibrated for 10 mins at each temperature.[1]

2.3. Analysis of SANS data

For a system of monodispersed interacting particles, the differential scattering cross-section per unit volume ($d\Sigma/d\Omega$) may be expressed as a function of scattering vector Q as:

$$\frac{d\Sigma}{d\Omega} = n\,(\rho_m - \rho_s)^2\, V^2\, [\langle F(Q)^2\rangle + \langle F(Q)\rangle^2 (S(Q)-1)] + B \qquad (1)$$

where n is the number density of micelles, ρ_m and ρ_s are the scattering length densities of the micelle and the solvent, respectively, and V is the volume of the micelle. F(Q) denotes the single-particle form factor which is the characteristic of specific size and the shape of the scatterer, and S(Q) denotes the interparticle structure factor. B is a constant, which represents the incoherent scattering background. The F(Q) is calculated by treating the micelles as prolate ellipsoids, using the equations: [2]

$$\langle F(q)^2\rangle = \int_0^1 [F(q,\mu)]^2\, d\mu \qquad (2)$$

$$\langle F(q)\rangle^2 = \int_0^1 [F(q,\mu)\, d\mu]^2 \qquad (3)$$

$$F(q,\mu) = \frac{3(\sin x - x\cos x)}{x^3} \qquad (4)$$

$$x = q[a^2\mu^2 + b^2(1-\mu^2)} \qquad (5)$$

where a and b are the semimajor and semiminor axes of an ellipsoidal micelle, respectively, and μ is the cosine of the angle between the directions of a and the wave vector transfer Q. The interparticle structure factor S(Q) identifies the correlation between the centers of different micelles, and it is the Fourier transform of the radial distribution function g(r) for the mass centers of the micelle. S(Q) is calculated using expressions derived by Hayter and Penfold from the Ornstein-Zernike equation and using the rescaled mean spherical approximation.[3] To simplify the calculation of S(Q), the micelle is assumed to be a rigid equivalent sphere of radius $\sigma = (ab^2)^{1/3}$ interacting through a screened Coulomb potential.

3. Results and Discussion

3.1. Surface activity of aromatic π systems and their influence on surface and bulk properties of cationic surfactants

The influence of head group architecture of the cationic surfactants CTAB and CPB on their interaction with the aromatic π conjugated hydroxy naphthalenes viz., 1 Naphthol, 2 Naphthol and 2,3 Dihydroxynapthalene (2,3 DHN) is studied via conductometry. Upon addition of the hydroxy aromatic derivatives, there is a gradual decrease in the cmc values of both CTAB and CPB. While 1 Naphthol lowers the cmc of the surfactants in a linear fashion (Figure 1(a)), a non-linear or exponential trend is exhibited by both 2 Naphthol and 2,3 DHN as a function of concentration, which is more prominent in the case of CPB. Moreover, it is striking that the cmc of CPB is lowered to a greater extent compared to the others, i.e., CTAB. The lowering of cmc values indicates that the micellization of both the cationic surfactants are facilitated due to presence of the additives.

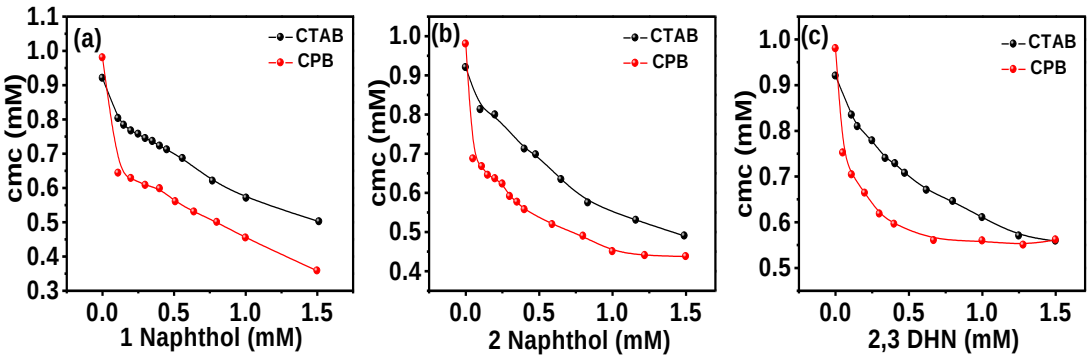

Figure 1. Variation of cmc of the surfactant-additive systems as function of (a) 1 Naphthol, (b) 2 Naphthol and (c) 2,3 DHN concentration at 303 K.

In a similar study, influence of phenol on micellization characteristics of CTAB have been reported previously.[4] A gradual decrease in cmc of CTAB was observed with increase in phenol concentration. The cmc of CTAB decreased from 0.93 mM in aqueous solution to 0.63 mM in presence of 10 mmol.kg^{-1} phenol. It was concluded that the decrease is cmc values was due to decreased electrostatic repulsion between the cationic head group of the CTAB micelle and salting out of the surfactant monomers. In the present study, it is evident that the lowering of cmc of CTAB as well as CPB occur at much lower concentration of the naphthalene derivatives. This stronger synergism may be attributed to the presence of the extra benzene moiety in the hydroxy naphthalene molecules and the extended conjugation therein.

In the present study, it is evident that the lowering of cmc of CTAB as well as CPB occur at much lower concentration of the naphthalene derivatives. This stronger synergism may be attributed to the presence of the extra benzene moiety in the hydroxy naphthalene molecules and the extended conjugation therein. In another study on Cetylpyridinium chloride (CPC)-Phenol interaction at different pH, it was found that at lower phenol concentration (0.5 mM, 1.0 mM), phenol was solubilized at the micelle-water interface driven by the interaction between the phenolate ion ($C_6H_6O^-$) and the pyridinium cation ($C_5H_5N^+$).[5] At higher phenol concentration (>2 mM), upon saturation of the micelle-water interface, $C_6H_6O^-$ is intercalated deeper into the palisade layer of the micelles. In the present case, the additives (aromatic π systems) remain in their protonated form, since the solution pH was maintained in the range 6.8-7.2 which is far below the pKa of the individual additives (viz., pK_a of 1 Naphthol is 9.34, pK_a of 2 Naphthol is 9.51, pK_a of 2,3 DHN is 9.10)[6] yet, they strongly interact with the surfactants thereby reducing the electrostatic head group repulsion between the cationic head groups and facilitating micellization. It is evident that interaction between the naphthalene moieties is stronger with CPB compared to that in CTAB, possibly due to the aromatic head group architecture of the latter. To obtain the composition of optimum interaction, the cmc of the systems are measured as function of different surfactant:additive molar ratios and displayed in Figure 2.

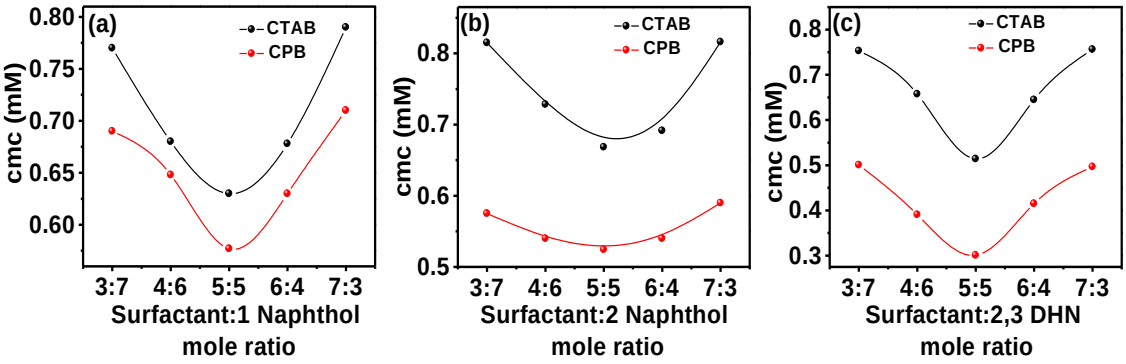

Figure 2. Variation of cmc of surfactant-additive systems at different surfactant:additive mole ratio, at 303 K.

It may be seen that for both CTAB and CPB, minimum value of cmc is obtained at equimolar composition of the surfactant and the respective additives. Theoretical calculations based on regular solution theory,[7] showed a similar cmc-concentration profile for mixtures of ionic and non-ionic surfactants with similar head group sizes.[8] The electrostatic free energy of mixing as a function of reduced charge density, S, assuming S>>1 have been expressed as:[8]

$$S = \frac{\sigma}{\sqrt{c_t.\epsilon_0\epsilon_r N_A kT}} \qquad (6)$$

Where, $\sigma = \frac{e_{el}}{a_{ch}}$ is the surface charge density, e_{el} is the elementary charge and $a_{ch}$is the area per charge at the aggregate surface. ϵ_0 and ϵ_r are the electric permeability in a vacuum and the relative permeability, respectively, N_A is the Avogadro constant, *k* is the Boltzmann constant and *T* is the temperature. Therefore, the synergistic effect observed between CTAB/CPB and the additives is due to electrostatic interaction governed by entropy of mixing of the surfactant and additive molecules with the solvent and as well as among themselves.[8] The increase in the cmc values beyond equimolar composition may be due to the self-interaction between the surfactants and thus becomes predominant at higher surfactant compositions and over-rules the synergism between surfactant and the additive.[9]

More insight on the strength and nature of interaction between the two components of the mixed systems is found out by calculating the interaction parameter, β, obtained on the basis of Rubingh's Regular solution theory.[10] According to this theory, the excess energy of mixing of the components in a mixed surfactant system is zero. The parameters viz., mole fraction of surfactant CTAB or CPB, α_1, experimental critical

aggregation concentration of the mixed system of the mixture, cac, critical aggregation concentration of CTAB, cac_1 (the cmc of CTAB in the mixed systems is now renamed as cac) and mole fraction of the surfactant within the micelles, X_1, are related as follows:[11]

$$\beta = \frac{\ln\{(cac.\alpha_1)/(X_1.cac_1)\}}{(1-X_1)^2} \quad (7)$$

X_1 is evaluated iteratively using the relation:[11]

$$\frac{[X_1^2.\ln(cac.\alpha_1/cac_1.X_1)]}{(1-X_1)^2}\ln\left[\frac{cac\,(1-\alpha_1)}{cac_2(1-X_1)}\right] = 1 \quad (8)$$

The respective activity coefficients f_1 and f_2 of the surfactant and respective hydrotopes are related to β as:

$$f_1 = \exp\{\beta\,(1-X_1)^2\} \quad (9)$$

$$f_2 = \exp\{\beta\,.{X_1}^2\} \quad (10)$$

All the π-conjugated additives viz., 1 Naphthol, 2 Naphthol and 2,3 DHN are reported to be surface active with well-defined critical aggregation values (Discussed in detail in Chapter IV). Therefore the surfactant-additive systems in the present study have been treated as mixed surfactant systems and the interaction between the head groups of the surfactant components are evaluated (Table 1). It is noteworthy that negative values of β are obtained for all the surfactant-additive systems implying that their interaction is essentially attractive and synergistic in nature. The hydroxy aromatic compounds interact more strongly with the aromatic pyridinium head group of CPB compared to quaternary ammonium head group of CTAB as evident from higher negative values of β observed for the CPB-additive systems at all the compositions (Table 1 as well). This result corroborates the lower cmc values observed in CPB-2,3 DHN system (Figure 2(c)). Moreover, among all the systems, the extent of head group interaction is the highest in between CPB and 2,3 DHN and lowest in between CTAB-2 Naphthol system. Most of the systems exhibit maximum value in β at or near the equimolar composition (except CTAB-2,3 DHN system and CPB-2 Naphthol system) implying that in most of the systems, entropically this composition is more favored compared to the others.

Table 1. Interaction parameter (β), activity coefficients (f_1 and f_2) of CTAB and CPB with 1-Napthol, 2-Napthol and 2,3 DHN at 303 K (Prefix 1 indicate surfactant, 2 indicate additive).

CTAB												
α_{Surf}	1-Napthol				2-Napthol				2,3 DHN			
actant	cmc	β	f_1	f_2	cmc	β	f_1	f_2	cmc	β	f_1	f_2
0.3	0.77	-4.14	0.06	0.27	0.81	-3.37	0.09	0.37	0.75	-3.49	0.08	0.37
0.4	0.68	-4.11	0.07	0.24	0.73	-3.41	0.11	0.32	0.66	-3.45	0.09	0.34
0.5	0.63	-4.11	0.08	0.21	0.66	-3.46	0.11	0.27	0.51	-4.49	0.05	0.21
0.6	0.68	-3.78	0.12	0.18	0.69	-3.31	0.15	0.24	0.64	-4.76	0.08	0.11
0.7	0.79	-2.66	0.29	0.24	0.81	-2.32	0.34	0.29	0.75	-2.59	0.27	0.27
CPB												
	cmc	β	f_1	f_2	cmc	β	f_1	f_2	cmc	β	f_1	f_2
0.3	0.69	-4.72	0.04	0.24	0.57	-5.03	0.03	0.24	0.50	-5.01	0.02	0.27
0.4	0.65	-4.43	0.05	0.22	0.54	-4.81	0.04	0.22	0.39	-5.77	0.02	019
0.5	0.57	-4.86	0.05	0.16	0.52	-4.75	0.05	0.19	0.30	-6.69	0.11	0.12
0.6	0.63	-5.53	0.05	0.08	0.54	-4.35	0.07	0.19	0.41	-5.44	0.03	0.14
0.7	0.71	-3.57	0.16	0.17	0.59	-3.87	0.11	0.18	0.49	-4.56	0.07	0.15

3.2. Nuclear magnetic resonance (NMR) study

3.2.1. ^{1}H NMR

To ascertain the location of the solubilized additives within the surfactant micelles, ^{1}H NMR study is undertaken. The molecular architecture of the additives viz., 1 Naphthol, 2 Naphthol and 2,3 DHN are similar, differing only in the position of the OH functionality in the aromatic ring. The hydroxy proton being labile, does not provide signals which could be worthwhile for NMR analysis. Therefore, the study is focused on determining the location of residence of the aromatic naphthalene ring with respect to the surfactant molecules. The collective ^{1}H NMR spectra of 2 Naphthol in D_2O, CTAB in D_2O and mixture of 10 mM CTAB and 10 mM 2 Naphthol in D_2O, alongwith the respective proton numbering, are presented in Figure 3. The spectra exhibit several interesting features. Firstly, considering the resonances for the aromatic moiety, it may be seen that the signals of 2 Naphthol in D_2O appear highly spilt displaying the most downfield and most upfield resonances at 7.86 and 7.18 ppm respectively (Figure 3(a)). However, in the CTAB-2 Naphthol mixture (Figure 3 (c)), the aromatic proton signals

are broadened and appear heavily merged and shielded, the most downfield and upfield resonances being at 7.46 and 7.06 ppm respectively. This upfield shift essentially imply a non-polar environment around the aromatic protons.[12] The broadening of signals are indicative of possible hydrogen bonding associated with the protons.[12] Secondly, the N-methyl protons of CTAB (C1) which normally resonate at 3.11 ppm in D_2O, also appear greatly shifted to lower ppm value i.e., 2.78 ppm ($\delta_{initial} - \delta_{final} = \Delta\delta = 0.33$ ppm).

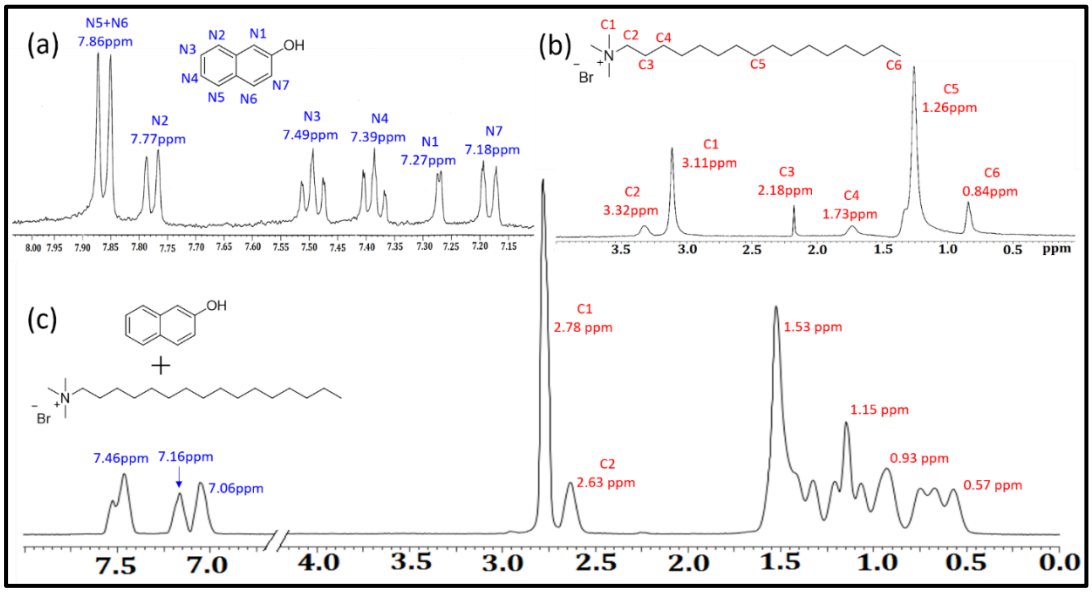

Figure 3. ^{1}H NMR spectra of (a) 5 mM 2 Naphthol in D_2O, (b) 10 mM CTAB in D_2O and (c) mixture of 10 mM CTAB and 10 mM 2 Naphthol in D_2O, at 298 K.

The most significant upfield shift is observed in the C2 protons, $\Delta\delta = 0.69$ ppm.[13] The resonances for the alkyl chain protons viz., C3, C4 and C5 as well as the terminal protons viz., C6, merge together and appear as multiplet ranging from 1.53 ppm to 0.57 ppm. It is striking that the intense signal corresponding to C5 protons appears at 1.26 ppm in D_2O (Figure 3 (b)), while in the CTAB-2 Naphthol mixture (Figure 3(c)), it appears at 1.53 ppm i.e., a downfield shift of $\Delta\delta = -0.27$. A similar upfield shift in the NMe (C1) as well as C1 and C2 proton resonances of CTAB has been reported in presence of phenol which has been shown to be the evidence in favor of radial penetration of the aromatic ring of phenol into the palisade layer of the CTAB micelles.[4] The presently observed shielding effect on the CTAB protons, may, therefore, be thought to be induced by the effect of ring current of the naphthalene ring of 2 Naphthol, which intercalates into the palisade layer and its location remains in the vicinity of the CTAB head group.[14,15] The huge perturbation of the alkyl proton resonances (Figure 3(c)) demonstrates interaction between naphthalene ring and the chain protons and this

further suggests much higher penetration depth of 2 Naphthol compared to that of phenol.[4] This leads to the concomitant upfield shift in the aromatic resonances. Intercalation of the extended benzene ring into micelle causes the hydrocarbon chains of CTAB to mutually move away apart causing an increase in the spatial distribution of the alkyl protons creating a relatively less non-polar environment in the vicinity which ultimately resulted in the downfield shift of the C5 resonances.[4,16]

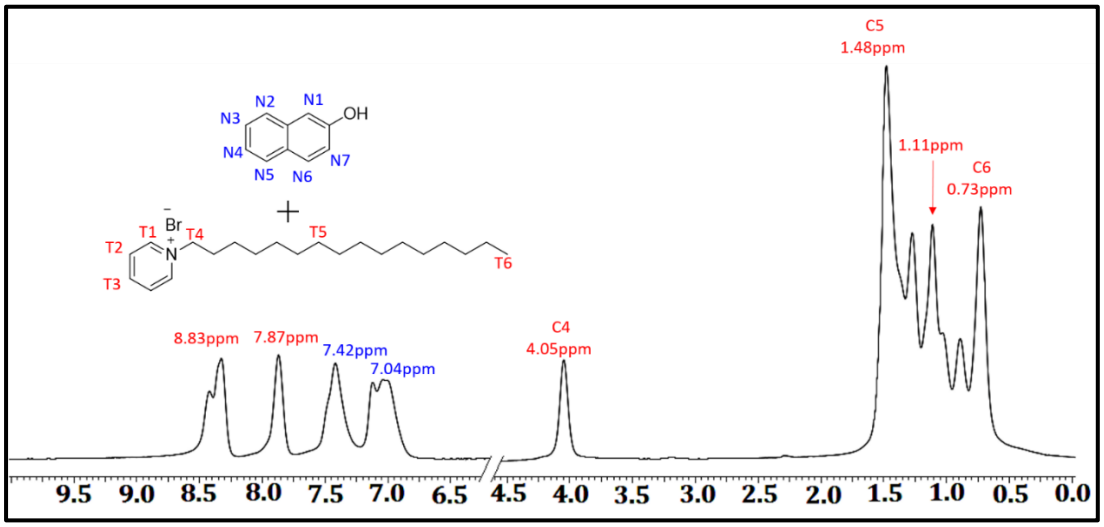

Figure 3 (d). ^{1}H NMR spectra of mixture of 10 mM CPB and 10 mM 2 Naphthol in D_2O, at 298 K.

The aromatic resonances for the pyridinium moiety of CPB in D_2O resonate highly downfield, in between 8-9 ppm[5] but in the CPB-2 Naphthol system (Figure 4 (d)), a merged broad peaks appear within 7.04 ppm to 8.83 ppm due to resonances of aromatic protons of both CPB and 2 Naphthol. It is apparent that the more downfield resonance is exhibited by pyridinium protons due to stronger deshielding of the same.[5] Therefore, a qualitative assignment of the aromatic resonances has been presented in Figure 5(d). The spectral line width of the aliphatic proton signals of CPB in the CPB-2 Naphthol mixed system is high, and these appear as multiplets, because of which specific assignment of proton resonances becomes less straightforward in this case. 2D NMR is, therefore, applied for achieving better insight on the molecular interactions.

3.3.2. NOESY

Nuclear Overhauser effect spectroscopy (NOESY) is a 2D NMR technique which presents correlation via dipolar interaction, between protons which are closer than 5 Å in space. Intensity of NOESY cross-peaks is a direct measure of extent of magnetization transfer and the internuclear distance between the protons.[17] The NOESY spectrum of

(10 mM) CTAB and (10 mM) 2 Naphthol and that of (10 mM) CPB and (10 mM) 2 Naphthol shows several cross-peaks correlating CTAB and the aromatic protons of 2 Naphthol as well as that of CPB and the aromatic protons (Figure 4).

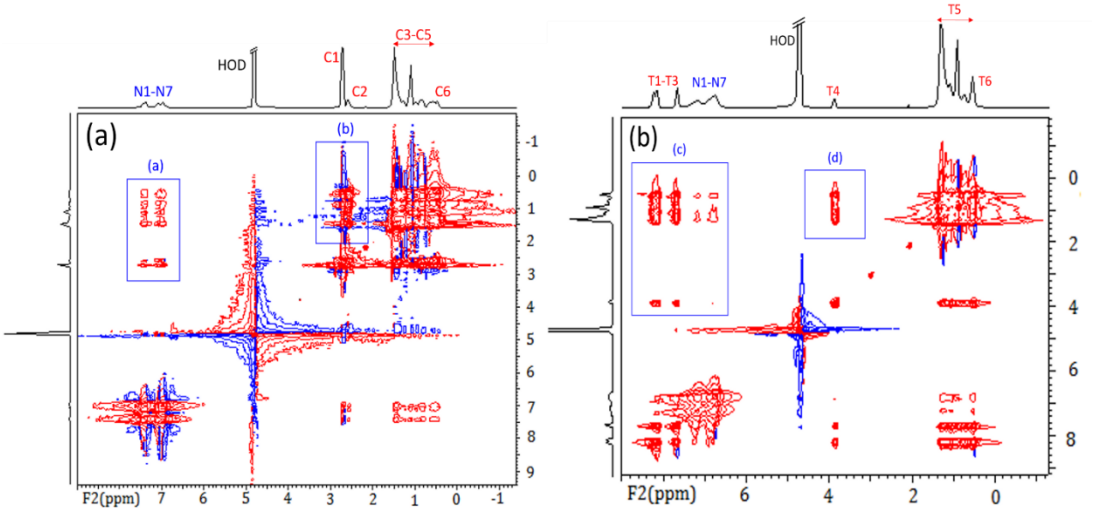

Figure 4. 2D NOESY spectrum of (a) 10mM CTAB and 10 mM 2 Naphthol in D_2O and (b) 10mM CPB and 10 mM 2 Naphthol in D_2O at 303 K.

The intense cross-peak N1-N7/C4 highlights the correlation between the NMe protons of CTAB with that of the aromatic ring. The presence of cross-peaks N1-N7/C1 and N1-N7/C2 (highlighted in the box (b) in Figure 4 (a)) which correlates the quaternary ammonium protons of CTAB with the terminal as well as some other aliphatic protons of the same is indeed interesting. This is indicative of apparent self-interaction within the CTAB molecule, which generally occur if the molecule remain in highly coiled conformation. This is, however, not likely to occur in our present system because of the presence of strong hydrophobic interactions between the hydrocarbon chain and the naphthalene moiety, indicated by the intense cross-peaks viz., N1-N7/C5-C6 which correlate the NMe protons as well as the chain protons of CTAB with the aromatic ring of 2 Naphthol (highlighted in box (a) in Figure 4(a)). This observation indicates the simultaneous proximity of the aromatic protons with the chain protons as well and provides evidence in favor of much deeper intercalation of the naphthalene moiety towards the micellar core as suggested from the ^{1}H NMR study.[4] Therefore, the apparent self-interaction between the head group and chain protons of CTAB is likely to originate from different CTAB molecules with different orientations. In all probabilities, this may occur near the end-cap regions of the rod/worm-like micelles. In

the case of CPB, cross-peaks indicating correlation between the aromatic protons of both 2 Naphthol (N1-N7) and CPB (T1-T3) with the α methylene protons of CPB (T4) are evident. Contrary to that observed in the case of CTAB, intensity of the N1-N7/T4 cross-peak is significantly less, which suggests a greater distance between the T4 and N1-N7 protons. Moreover, key cross-peaks indicating interaction between the alkyl and terminal protons with the naphthalene as well as pyridinium moiety, is apparent (Highlighted in box (c)), although intensity corresponding to interaction with 2 Naphthol is relatively low. Moreover, similar to that observed in the case of CTAB-2 Naphthol system, the self-interaction between the T4 and the T5-T6, is also apparent in CPB-2 Naphthol system.

The origin of the observed interactions in NOESY spectra may be understood by considering the different forces operating within the systems. Spectroscopic investigations of CTAB-1 Naphthol system in aqueous solutions has revealed that naphthols have the unique ability to form hydrogen bonds with the interfacial water molecules at its vicinity, in which the proton atoms of its hydroxy groups act as the donors.[12] This is considered as the driving force behind the embedding of the 2 Naphthol molecules in between the CTAB monomers within its micelle. A similar argument may be adopted to explain the observed interactions in the present CTAB-2 Naphthol system. The restructuring of water molecules at the micelle-water interface causes the OH functionality of 2 Naphthol to orient outward from the micellar interface, while the aromatic rings are embedded in between head groups of CTAB. 2D ROESY analysis show that this orientation is favored by strong cation-π interaction between the quaternary ammonium head group and the π-electron cloud of the naphthalene moiety and also by hydrophobic interactions between the aromatic protons and the alkyl chain protons.[12,18,19] This interaction largely neutralizes the positive charge on head group of CTAB monomers and facilitates micellization which is reflected in the conductometric study. The π-π interactions, on the other hand, are known to control diverse phenomenon like stabilization of the DNA double helical structure,[20] tertiary structure of proteins,[21] packing of aromatic molecules in crystal,[22] etc. This interaction results if the attractive interaction between π-electron and σ- framework outweigh the repulsive interaction between two π-electron system.[23] CPB is essentially an electron deficient aromatic system with a positively charged nucleus surrounded by delocalized π-electron cloud, while 2 Naphthol is a neutral electron rich aromatic system with

extended π-electron conjugation. The CPB-2 Naphthol system is likely to be dominated by the π-π interaction instead of the cation-π interaction as observed in CTAB-2 Naphthol system.[20] The electrostatic complementarity between the π-electron rich 2 Naphthol and the π-electron deficient CPB head group can lead to strong face-to-face stacking and thereby screening the head group charge of the CPB molecule because of which the micellization is favored.[24] Due to this interaction along with the rigid anchoring of the OH moiety to the interfacial water and further due to the larger head group size of pyridinium ring, the naphthalene moiety does not penetrate deep inside the micelle for which the relatively less intense cross-peaks correlating the aromatic naphthalene protons and CPB chain protons are observed in the NOESY spectra (Figure 3 (b)). A schematic representation of the molecular orientation in the CTAB-2 Naphthol and CPB-2 Naphthol systems is proposed in Scheme 1. Due to stronger cation-π interaction, the naphthalene additive shield the electrostatic charge of the CTAB head groups more efficiently, compared to π-π interaction which is further corroborated in the SANS study (Discussed later).

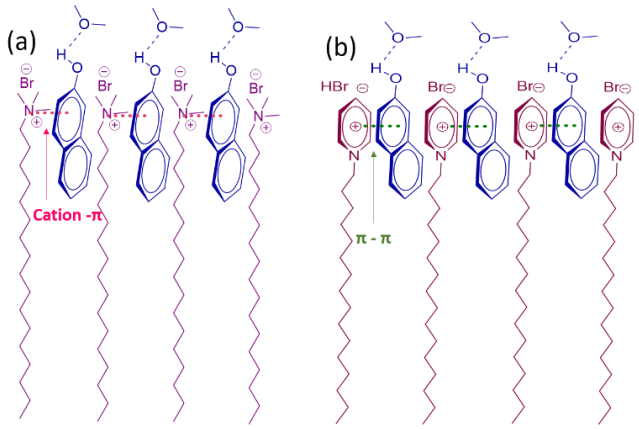

Scheme 1. Schematic representation of possible molecular orientation in the (a) CTAB-2 Naphthol system and (b) CPB-2 Naphthol system.

Due to the effective shielding of the head group charges via intercalation of the naphthalene moiety in between the surfactant monomers in micelles, the effective head group area, a_0, of the surfactant is decreased, which eventually increase the packing parameter, P of the surfactant. P governs the aggregate morphology and is given by:[25]

$$P = \frac{v}{a_o.l_c} \tag{11}$$

where ν and l_c are the volume and the extended length of the surfactant tail, respectively. For spherical micelles, $P > \frac{1}{3}$, while for elongated or worm-like micelles,

$\frac{1}{2} > P > \frac{1}{3}$.[25] The ellipsoidal or wormlike micelles in the present surfactant-additive systems are thus formed as the consequence of the electrostatic shielding of the head group charge.[26] To minimize the end cap energy, long wormlike micelles are formed with cylindrical body and nearly spherical end caps. Due to spatial congestion near the endcaps and higher density of the surfactant molecules, intermolecular interaction between the surfactants are likely to be predominant at the end cap and this may be responsible for the corresponding cross-peaks observed in the NOESY spectrum (Figure 4(a), (b)) as mentioned before. These aspects have been discussed in further detail in Chapter VI.

3.3. Small angle neutron scattering (SANS) study

The structural aspects of surfactant aggregates in solution may be obtained via SANS study.[27] In a SANS experiment, the sample is subjected to a beam of neutrons and the intensity of the scattered neutrons are measured in different directions. To obtain larger scattering intensity, samples are made in deuterated solvents. The SANS profile of the surfactant-additive systems are provided in Figure 5. The SANS spectra of the surfactant in the presence of the additives show a rise in the low Q region, while scattering in the high Q region is independent of the surfactant type and is nearly identical for CTAB and CPB in case of all the additives. The SANS spectra of CTAB in D_2O[26] and CPB in D_2O[28] show a characteristic correlation peak at the intermediate Q region, signifying the presence of inter-particle electrostatic interaction. In presence of 1 Naphthol, no correlation peak is evident in either CTAB or CPB (Figure 5 (a)) which demonstrates that the electrostatic repulsions between the charged head group of CTAB as well as CPB is efficiently reduced due to the presence of 1 Naphthol.[26] There is a rise in intensity at the low Q region for CTAB compared to CPB, in case of all three additives which signifies a growth in the micellar structure for CTAB compared to CPB in all the three cases.[2]

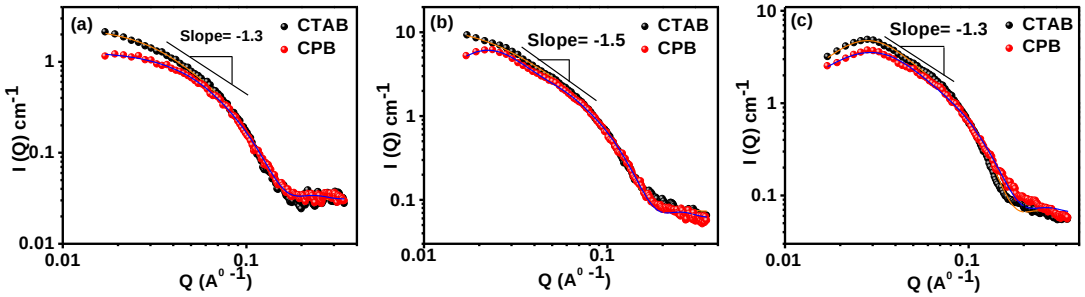

Figure 5. SANS distribution profile of 25 mM CTAB and 25 mM CPB in the presence of (a) 25 mM 1 Naphthol, (b) 25 mM 2 Naphthol and (c) 25 mM 2,3 DHN at 303 K. Solid circles represent experimental curve, solid lines represent theoretical fit for prolate ellipsoid micelle model.

The spectra of CTAB in presence of 2 Naphthol (Figure 5 (b)) is similar to that in the presence of 1 Naphthol, while, a correlation peak is evident in spectra of CPB meaning that electrostatic repulsion is present in this system, i.e., the screening of CPB head group repulsion by 2 Naphthol is less efficient than that in the case of CTAB. In presence of 2,3 DHN, distinct correlation peak is evident for CTAB and CPB (Figure 5 (c)). The peak appear at higher Q value for CPB compared to 2 Naphthol. The correlation peak generally occur at $Q \approx \frac{2\pi}{d}$, where d is the average distance between the aggregates present in the sample.[2] Thus, the observation imply a decrease in correlation length in the surfactant-2,3 DHN systems, ξ, given by $\xi = 2\pi/Q_{max}$.[26] The nearly identical Q_{max} for CTAB and CPB (Figure 5 (c)) imply that aggregate density in both the systems is identical. The SANS data are fitted to the prolate ellipsoid micellar model and it is found that the model is in excellent agreement with the experimental curves (Solid lines in Figure 5). This interestingly signifies that a structural modification of the spherical micelles of both CTAB and CPB is mediated by the hydroxy aromatic derivatives. The slope of the intensity vs Q at the intermediate Q region is obtained as -1.3, -1.5 and -1.3 for 1 Naphthol, 2 Naphthol and 2,3 DHN respectively and may be taken as an indication of presence of wormlike or rod like structures in the system.[28] Table 2 represents the structural dimension of the surfactant-additive systems obtained on fitting the experimental data to prolate ellipsoidal micellar model.

Table 2: Dimension of wormlike micelles of CTAB and CPB in presence of 1 Naphthol, 2 Naphthol and 2,3 DHN at 303 K, as obtained from SANS study.

	CTAB		CPB	
	Semi minor axis (Å)	Semi major axis (Å)	Semi minor axis (Å)	Semi major axis (Å)
1 Naphthol	23	92	22	59
2 Naphthol	26	122	21	110
2,3 DHN	22	74	19	72

It is apparent that the micelles of the system are rod like having length about five times of the radius. Longest worm like micelles are formed in CTAB-2 Naphthol system while shortest worms are formed in CPB-1 Naphthol system. Nevertheless, the result indicate that the hydroxy aromatic derivatives steer the transition of morphology of spherical aggregates of both CTAB and CPB, to elongated worm like.

3.4. Rheology of the wormlike micelles

On minimizing head group repulsion, surfactant micelles are capable of forming linear wormlike aggregates which have characteristic property of a viscoelastic gel, i.e., these giant molecules can withstand external stress up to a critical extent (Newtonian behavior) beyond which they become viscous or fluid-like.[29] Rheology is an important tool to measure the viscoelastic traits of such systems. On the application of an external stress, the system undergoes deformation followed by relaxation in order to regain its equilibrium state. According to the living polymer model of Cates[30] the relaxation of the viscoelastic micelles involves two time scales viz. reptation time (τ_{rep}) corresponding to curvilinear diffusion of a chain along its own contour and breaking time (τ_b) which is the result of chain scission. When $\tau_b << \tau_{rep}$, there occurs many breakages and recombination before the chain segment relaxes by reptation. The system is then defined by a single stress relaxation time, τ_R, given by $\tau_R=(\tau_{rep.}\ \tau_b)^{1/2}$ and is characterized as a Maxwell Fluid. The sinusoidal deformation on the system, at an angular frequency ω, causes the response stress, which remains out of phase with the applied strain.

The sinusoidal deformation (strain, $\gamma(t)$) can be expressed as:

$$\gamma(t) = \gamma_0 \exp(i\omega t) \tag{12}$$

where, γ_0 is the amplitude of the strain, ω is the angular frequency and t is the time.

The response stress will also be sinusoidal and will have a phase difference of δ, i.e.

$$\sigma(t) = \sigma_0 \exp(i[\omega t + \delta) \quad (13)$$

The complex modulus (G*) thus obtained is defined as:

$$G^* = \frac{\sigma(t)}{\gamma(t)} = \frac{\sigma_0 (cos\delta + isin\delta))}{\gamma_0 \exp(i\omega t)}$$

or, $G^* = G' + iG''$ (14)

where G' is the storage modulus and G'' is the loss modulus and these reflect the respective extent of elastic and viscous property of the system. For a fluid with near-Maxwell character, the elastic (or storage modulus), G' and viscous (or loss modulus), G'' are related to angular frequency, ω as: [31]

$$G'(\omega) = \frac{G_0 \omega^2 \tau_R^2}{(1+\omega^2 \tau_R^2)} \quad (15)$$

$$G''(\omega) = \frac{G_0 \omega \tau_R}{(1+\omega^2 \tau_R^2)} \quad (16)$$

where G_0 is the storage modulus at high frequency, where it exhibits a plateau, also called the plateau modulus. It is proportional to the number density of the entanglement points and hence characterize the network structure.[32] τ_R is obtained from inverse of crossover frequency, i.e. the frequency where G' and G'' intersects. Furthermore, Cole-Cole plot i.e the plot of G'' *v/s* G' is expected to yield a semicircle at low frequency region for a Maxwell fluid.[31]

3.4.1. Dynamic oscillatory measurements

Oscillatory measurements were carried out to characterize the flow behavior of the viscoelastic gels. Figure 6 presents the variation of G' and G'' with ω, for the surfactant-additive systems at different temperature. The response of G' and G'' as function of ω is typical to that observed in viscoelastic fluids comprised of wormlike micelles.[26,32,33] At lower ω, systems are predominantly viscous with G″ predominating over G′ while at high ω, G′ > G″ and the systems exhibit elastic behavior. There exists a distinct cross over point, ω_c, at which $G' = G''$. With rise in temperature, the frequency spectra shifts to the right, exhibiting higher ω_c.

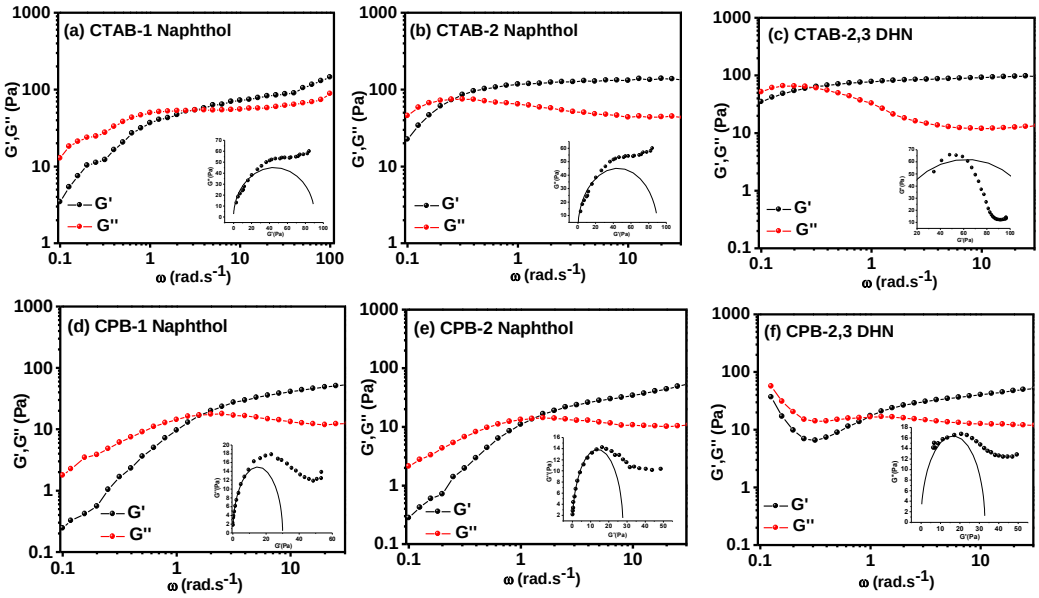

Figure 6. Dynamic viscosity profile of (a) 100 mM CTAB-100 mM 1 Naphthol, (b) 100 mM CTAB-100 mM 2 Naphthol, (c) 100 mM CTAB-100 mM 2,3 DHN, (d)100 mM CPB-100 mM 1 Naphthol, (e) 100 mM CPB-100 mM 2 Naphthol and (f) 100 mM CPB-100 mM 2,3 DHN at 328 K. Insets display the respective Cole-Cole plots.

A higher value of ω_c imply lower relaxation time, τ_R, as $\tau_R = {}^{1}/_{\omega_c}$.[34] The variation of τ_R as function of temperature (Figure 7) shows that the wormlike micellar systems composed of CTAB-additive (2 Naphthol and 2,3 DHN) relaxed relatively slower (or higher values of τ_R) compared to CPB-additive system (2 Naphthol and 2,3 DHN).

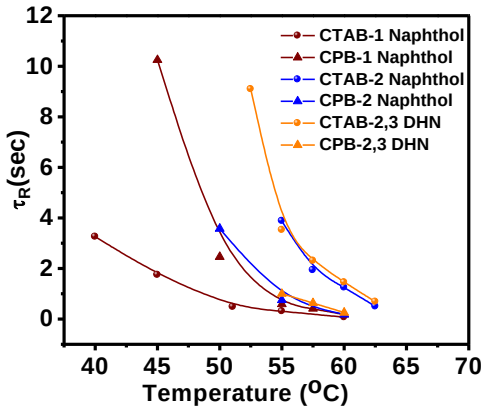

Figure 7. Variation of τ_R with temperature for different surfactant-additive systems.

The network mesh size of the entangled wormlike micelles is characterized by ξ the hydrodynamic correlation length. This length scale can be obtained directly from the plateau modulus G_0: [35]

$$\xi = (\frac{k_B.T}{G_0})^{1/3} \quad (17)$$

ξ is related to the persistence length,l_p, of the micelles and the entanglement length, l_e the average distance along the micelle between two entanglement points in the micellar network as:

$$l_e = \frac{\xi^{1/3}}{l_p^{2/3}} \quad (18)$$

The entanglement length can be determined from measurements of viscoelasticity using:[30]

$$\frac{G_0}{G''_{min}} = \frac{L_{avg,}}{l_e} \quad (19)$$

where $L_{avg,}$ is the average micelle length and G''_{min} is the local minimum of the G'' curve at frequencies above $1/\tau_R$. The ratio $L_{avg,}/l_e$ defines the average number of entanglements per micelle.

Table 3 summarizes the parameters obtained from rheological study of the surfactant-hydrotope systems. It is evident that in all the cases, $\tau_{br} << \tau_{Rep}$, which characterizes all the systems with a single relaxation time i.e., they exhibit Maxwellian behavior in the concerned temperature range.

Table 3 shows that the τ_{Rep} of CTAB-2 Naphthol system varies from ~284 sec to 0.38 sec in temperature range 313-333 K whereas that in case of CPB-2 Naphthol varies within ~976 sec to 3 sec within same temperature range. In the case of CTAB-2,3 DHN system, τ_{Rep} ranges from ~1486 sec to 100 sec for a temperature jump of 5K from 328 K to 333 K whereas under similar conditions, τ_{Rep} for CPB-2,3 DHN system ~47 sec to 3 sec. A higher value of τ_{Rep} is indicative of slower relaxation, which is associated with linearity of the micellear framework,[31] i.e., longer micelles are formed in CTAB-2 Naphthol/2,3 DHN systems compared to CPB-2 Naphthol/2,3 DHN systems while 1 Naphthol shows the preference to form longer micelles with CPB compared to CTAB as evident from the higher values of τ_{Rep} in case of CPB (Table 3). Flow activation energy, E_A, which describes the end-cap energy and the energy required for reversible micellar scission and is regarded as a measure of the "compactness" or "slowness" of the WLM flow has been evaluated as:

$$\tau_R = A.\exp(E_A/R.T) \quad (20)$$

or, $\log \tau_R = \log A + ({}^{E_A}/_{R.T})$ (21)

where A is the pre-exponential factor and is a constant, R is the universal gas constant taken as 8.314 J.mol^{-1}. K^{-1} and T is the temperature.

Table 3. Parameters G''_{min}, $\tau_R, \tau_b, \tau_{rep}, \xi$, L as obtained from rheological data for 100 mM CTAB and 100 mM CPB with 100 mM 1 Naphthol, 100 mM 2 Naphthol and 100 mM 2,3 DHN as additive at different temperatures.

Additive	Temp K	G''_{min} Pa	τ_R s	τ_b s	τ_{rep} s	ξ x 10^6 m	L nm
1 Naphthol				CTAB			
	313	14.18	3.34	0.04	279.32	1.93	340-637
	318	50.78	0.59	0.01	284.11	1.63	158-297
	323	60.33	2.92	0.08	1.44	1.62	138-259
	328	56.82	3.30	0.08	1.55	1.71	127-238
	333	85.28	4.17	0.01	0.38	1.61	102-192
				CPB			
	318	4.63	0.10	0.10	975.86	2.14	766-1437
	323	7.34	0.41	0.05	119.10	2.16	482-903
	328	8.26	1.62	0.02	24.08	2.17	428-804
	330.5	8.36	2.52	0.02	9.92	2.15	435-816
	333	10.84	5.62	0.01	3.24	2.01	421-790
2 Naphthol				CTAB			
	328	43.57	3.88	0.010	1486	1.47	354-664
	330.5	58.61	0.27	0.012	6.08	1.45	202-379
	333	18.63	1.26	0.015	100.3	1.46	637-1195
	335.5	39.76	0.52	0.013	20.9	1.53	259-486
				CPB			
	323	5.09	3.66	0.06	213	2.00	872-1635
	328	6.96	0.77	0.01	47.45	2.01	641-1203
	333	10.43	0.18	0.01	2.82	2.01	427-801
2,3 DHN				CTAB			
	325.5	8.05	9.34	0.13	693.20	1.83	725-1359
	328	11.97	3.48	0.09	121.75	1.66	657-1233
	330.5	13.56	2.29	0.06	82.42	1.63	623-1168
	333	17.70	1.45	0.03	66.71	1.62	487-913
	335.5	23.43	0.67	0.02	28.56	1.88	237-444
				CPB			
	328	12.36	1.05	0.05	22.21	2.02	353-662
	330.5	5.27	0.64	0.13	3.23	2.05	799-1498
	333	17.61	0.26	0.063	1.07	2.29	225-423

Arrhenius' semilog plot of τ_R v/s temperature shows a straight line (Figure 8) implying a single exponential decrease in relaxation time with temperature. This further characterizes the system as Maxwell fluid.[31,36]

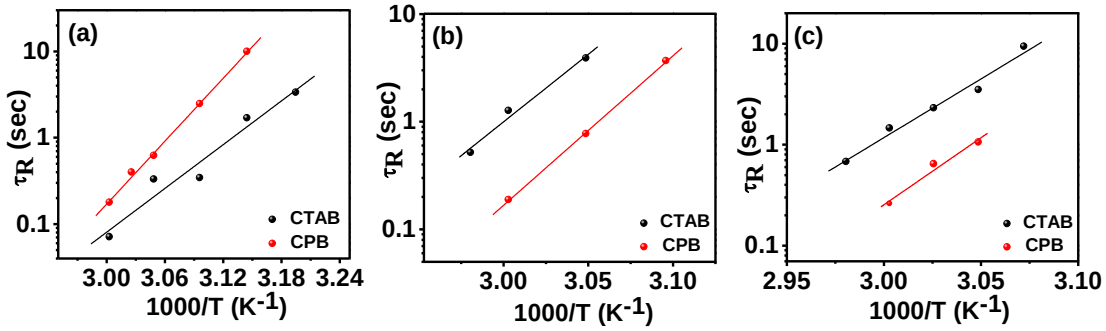

Figure 8. Arrhenius' Semi log plots of τ_R as function of inverse of temperature for 100 mM CTAB and 100 mM CPB in presence of (a) 100 mM 1 Naphthol, (b) 100 mM 2 Naphthol and (c) 100 mM 2,3 DHN for different surfactant systems (100mM ,1:1).

The flow activation energy for all the systems obtained following Equation 21, are summarized in Table 4.

Table 4. Flow Activation energies of different surfactant-additive systems obtained from Arrhenius' semi-log plots.

Flow Activation Energy, E_a (kJ.mole^{-1})			
Surfactant	1 Naphthol	2 Naphthol	2,3 DHN
CTAB	70.26	104.26	96.71
CPB	101.46	115.47	110.38

Results indicate that the wormlike micelles of CPB-additive systems possess a more flow activation energy compared to corresponding CTAB-additive systems implying that more compact micelles are formed in the former. Nevertheless, the study show that the architecture of surfactant head group can fine tune the molecular interaction and determine the specificity of additives towards forming wormlike micelles of desired length scale.

4.0. Conclusion

A synergistic interaction has been observed between the cationic surfactants (viz., CTAB and CPB) and the hydroxy aromatic compounds 1 Naphthol, 2 Naphthol and 2,3 DHN. As a result of reduction in electrostatic repulsion between the surfactant headgroups caused by the π-electrons of naphthalene additives, the cmc's of both

CTAB as well as CPB are lowered in presence of the aromatic compounds, nevertheless CPB displays a greater decrease in cmc compared to CTAB. 1H NMR and 2D NOESY study revealed that the hydroxynaphthalene derivatives intercalate deeper within the CTAB micelles while reside at the palisade layer of CPB micelles. Hydrogen bonding between the OH of the aromatic additives and the interfacial water molecules facilitate favorable orientation of the aromatic compounds to position within the surfactant micelles. 1 Naphthol most efficiently reduces the electrostatic repulsion between the surfactant head groups while 2,3 DHN is found to be least efficient in this respect. Furthermore, morphology transition of the surfactant aggregates from spherical to rod/ellipsoidal (at 25 mM surfactant:additive concentration) is also evident. At higher concentrations, (surfactant:additive >100 mM), the surfactant-additives systems formed thick viscoelastic gel consisting of long wormlike micelles (WLM). While 2 Naphthol and 2,3 DHN form longer micelles with CTAB, in the case of 1 Naphthol, longer micelles are formed with CPB. Moreover, WLM's of CPB are more compact than that of CTAB. This observed difference in rheological behavior probably originates from the difference in headgroup architecture of the surfactants. While strong cation-π interaction between the quaternary ammonium group of CTAB and the π electron cloud of the additives dominate the CTAB-additive systems, the CPB-additive are governed by the consequent π-π stacking between the aromatic pyridinium moiety and the naphthalene ring of the additives. Nevertheless, the study reveals high efficiency of the hydroxyaromatic compound viz., 1 Naphthol, 2 Naphthol and 2,3 DHN as effective triggering agents of morphology transition from spherical to wormlike micelles, under neutral salt-free conditions. The study also highlights the fact that WLM with fascinating rheological properties may be designed by tuning the headgroup architecture of surfactant and the nature of triggering agent under salt-free condition.

References are provided in BIBLIOGRAPHY under "References for Chapter III" (Page 170-172).